*J. Agr. Sci. Tech. (2017) Vol. 19: 1227-1240*

# Experimental Analysis of a Solar Dryer Equipped with a Novel Heat Recovery System for Onion Drying

H. Mortezapour[1*], S. J. Rashedi[1], H. R. Akhavan[2], and H. Maghsoudi[1]

## ABSTRACT

**In hot air dryers, only a small percentage of the provided thermal energy is used for the drying process, while a large fraction is lost via the exhaust air. To recycle waste heat from the exhaust air, the present study aimed to develop a solar dryer equipped with a novel heat recovery system. The designed dryer comprised of a solar air collector, a drying chamber, an internal closed-loop air circuit and an open-duct heat recovery system. The evaluation tests were conducted at different allowable relative humidities (RH) and mass flow rates of the recirculating air. The results indicated that the best solar fraction was at the highest RH and air flow rate. Increasing the *RH* from 7 to 17% caused a reduction of 51% in electricity consumption. Furthermore, electrical energy needed for drying increased by 24% with raising the air flow rate from 0.008 to 0.016 kg $s^{-1}$. A minimum specific energy consumption of 7.54 MJ $kg^{-1}$ was observed at the highest *RH* and the lowest air flow rate. At a constant RH, reduction of the air flow rate led to an increasing trend in lightness and decreasing trends in browning index of the products. Moreover, increasing the *RH* from 7 to 17% increased lightness and decreased browning index. In general, it can be stated that the best colour quality was achieved when the minimum air flow rate and the maximum *RH* were used for the solar drying.**

**Keywords**: Browning index, Energy recycling, Specific energy consumption, Surface colour.

## INTRODUCTION

Drying is a sophisticated process which needs a lot of energy. Solar drying is one of the most attractive methods for dehydration of agricultural products, especially in developing countries. Moisture removal from foods using solar dryers is usually a slow process impeded by intermittent and low solar radiation intensities as well as low energy efficiency of the traditional solar collectors. Recently, several researchers have attempted to present more efficient designs for solar collectors and use thermal storages, auxiliary heaters, and hybrid solar dryers to improve solar energy gain as well as drying time and capacity (Dina *et al.*, 2015; Elkhadraoui *et al.*, 2015; Fudholi *et al.*, 2015; Gudiño-Ayala and Calderón-Topete, 2014; Jain and Tewari, 2015; Shalaby and Bek, 2014). A desiccant bed was used for product drying during off sun-shine hours (Shanmugam and Natarajan, 2007). Türk Toğrul and Pehlıvan (2003) utilized an indirect forced convection solar dryer equipped with a conical solar concentrator for apricot dehydration. Similarly, Ringeisen *et al.* (2014) developed a dryer coupled with a concave solar concentrator for tomato.

In hot air dryers, only a small percentage of the provided thermal energy is used for

[1] Department of Mechanical Engineering of Bio-systems, Faculty of Agriculture, Shahid Bahonar University of Kerman, Kerman, Islamic Republic of Iran.
[*] Corresponding author; E-mail: h.mortezapour@uk.ac.ir
[2] Department of Food Science and Technology, Faculty of Agriculture, Shahid Bahonar University of Kerman, Kerman, Islamic Republic of Iran.

the drying process, while a large fraction is lost via the dryer walls and exhaust air. Therefore, recycling the waste energy associated with the exhaust air is an effective method to improve energy efficiency of the dryers. For this purpose, several researchers utilized dryers with partially recirculating air systems or employed desiccant beds, commonly silica gel, in closed-loop dryers. Das *et al.* (2001) developed a recirculating dryer and achieved a thermal efficiency of 22.16%. Sarsavadia (2007) suggested a solar dryer equipped with a recirculating air system for onion drying. The results showed that a maximum total energy saving of 70.7% can be achieved by recycling the exhaust air at drying temperature of 65 to 75°C. A hybrid photovoltaic-thermal solar dryer equipped with a silica gel desiccant was developed by Punlek *et al.* (2009). They indicated that the designed dryer can reduce drying time by 44% and lower energy consumption to 63% compared to hot air drying. Wannapakhe *et al.* (2012) reported an energy saving of 28.13% using a hot air dryer with a closed-loop oscillating heat pipe.

Another promising method for heat capturing from the moist exhaust air, which has been increasingly employed by researchers in the recent years, is heat-pump drying (Aktaş *et al.*, 2015; Hossain *et al.*, 2013; Mortezapour *et al.*, 2012; Şevik, 2014). A literature review indicates that heat pump dryers offer more energy-efficient systems and are especially beneficial to high quality and heat sensitive products.

Silica gel has a limited capacity (approximately 40% of its own weight) for absorbing humidity, so, when it soaks a certain amount of water, required a process to regenerate saturated desiccant. The regeneration stage is an energy- and time-consuming procedure. Furthermore, coupling a heat pump with the solar dryers makes a more sophisticated and complicated system which needs an external electrical supply to power heat pump compressor. The present study aimed to develop a solar dryer with a simple heat recovery combination using a recirculating air and a heat exchanger system for onion drying. A survey of the literature shows that similar solar dryer has not been used by previous researchers. Therefore, this study also aimed to investigate the effect of different drying conditions (relative humidity and air velocity) on the performance of the proposed solar dryer as well as surface colour variations of the dried onion slices.

## MATERIALS AND METHODS

### Theory and Working Principles

The proposed assembly recirculates the drying air in the dryer until its RH rises up to a set point; upper that, the dryer discharges the circulating air and utilizes the heat exchanger to transfer heat from the moist exhaust air to fresh inlet air. Since the moist air in the designed dryer can be completely replaced by dry fresh air, the system needs no desiccant chamber or heat pump system. A schematic of the designed solar dryer equipped with the proposed heat recovery system is demonstrated in Figure 1. The solar dryer is an indirect active type made up of a solar air collector, a drying chamber, an internal closed-loop air circuit, and an external heat recovery system. At the beginning of the process, drying air passes over the solar collector and, at a constant humidity ratio, its temperature increases getting heat from flat plate solar absorber. Air temperature rise in the solar collector is given by Equation (1) (Duffie and Beckman, 2006).

$$\Delta T_c = \frac{A_c F_R [I_t(\tau\alpha)_e - U_L(T_{ci} - T_a)]}{\dot{m}_{da} C_a} \quad (1)$$

The warm air passes through the product tray, and therefore its temperature decreases and its humidity ratio rises while the enthalpy can be assumed to remain constant. Hence, humidity ratio of air after drying stage can be calculated from the empirical equation presented by Brooker *et al.*

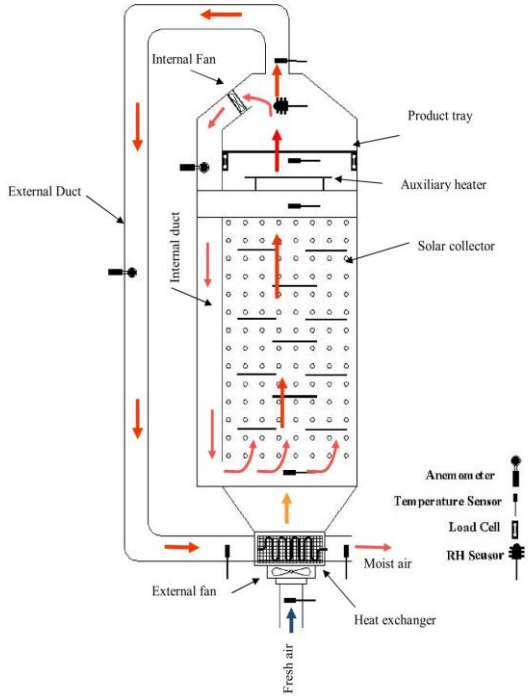


**Figure 1.** A schematic view of the solar dryer with the heat recovery system.

(1992).

$$\omega_{od} = \frac{h_{da}}{(2512131 + 1552.4\, T_{od})} - 1006.9\, T_{od}$$

(2)

After passing through the product tray, the approximately moist air circulates in the internal closed-loop system and returns to the collector inlet. This process continues until *RH* of drying air reaches its set point value. At this moment, a controller turns the external fan on to force the warm moist circulating air out of the dryer through the hot side of the heat exchanger and simultaneously takes fresh air inside the dryer via the cold side of the heat exchanger. This allows the cold fresh air to absorb a fraction of heat associated with the exhaust hot air in the heat exchanger before entering the solar collector. Heat transfer from the exhaust air to the fresh air can be obtained from Equation (3) (Incropera and DeWitt, 1996).

$$\dot{q}_{HE} = U_{HE} A_{HE} \Delta T_{lm}$$

(3)

Where, the overall heat transfer coefficient ($U_{HE}$) can be obtained by the following equation (Incropera and DeWitt, 1996).

$$U_{HE} = \frac{1}{\frac{1}{h_a \zeta_f} + \frac{A_{HE}}{A_i h_e} + \frac{A_{HE} \ln(\frac{D_o}{D_i})}{2\pi K_m L_t}}$$

(4)

The fresh air with low humidity ratio is then mixed with the circulating air coming from the internal closed-loop system. This makes humidity ratio of drying air to drop below the set point. Humidity of the mixture is given by Equation (5) (Brooker *et al.*, 1992):

$$\omega_m = \frac{\dot{m}_r \omega_r + \dot{m}_a \omega_a}{\dot{m}_r + \dot{m}_a}$$

(5)

## Experimental Setup

A photograph of the fabricated solar dryer is illustrated in Figure 2. The collector duct was constructed from 3 cm thick woods and insulated by glass-wool. Length, width, and depth of the collector were 130, 85, and 10 cm, respectively, and a tempered glass (5 mm thick) was used as the transparent cover. The absorber plate was made up of a black painted aluminium sheet (2 mm thick) on which a number of aluminium blades (2 mm thick and 250 mm long) with total surface area of 0.1 $m^2$ were embedded to act as the cross fins. Around 300 holes (diameter of 12 mm) were made on the absorber plate to achieve a perforated plate with the porosity of 0.03 (Zomorodian and Barati, 2010). The plate was installed obliquely inside the duct to ensure that all of the drying air passes through the holes. The collector was directly coupled to the drying chamber which was constructed from 3 cm thick woods and the sides were insulated by glass-wool. The auxiliary heater consisted of two electric

**Figure 2.** A photograph of the solar dryer equipped with the heat recovery system.

heater elements with a nominal power of 700W each and was installed at the inlet of the drying chamber.

The designed dryer had an internal closed-loop air system made up of an internal fan and a guide duct. A 12V battery was used to power the fan which was located above the crop tray where takes the air passed over the products and blows it down to the collector inlet.

Since *RH* of the recirculating air rises during the drying process, the open-duct heat recovery system was deployed to replace a fraction of the moist air with fresh air and reduce *RH* of drying air. The system consists of a 12V DC external fan, a thermally insulated duct and an air to air heat exchanger. The heat exchanger was a finned-tube type constructed from an oscillating tube with inner diameter of 2.5 cm and 28 fins with dimensions of 15×35 cm. The heat exchanger was installed in a wooden box covered with glass-wool.

## Experimental Procedure

The evaluation tests were carried out in Bio-systems Engineering Campus of Shahid Bahonar University of Kerman, Iran, during June 2016. To investigate the performance of the open-duct heat recovery system and solar collector efficiency a set of primary experiments were considered before the main tests. The trials were conducted at three levels of exhaust air temperature (55, 65, and 75°C) and a constant air flow rate of 0.012 kg $s^{-1}$.

In the main experiments, uniform slices of fresh onions were dried on a tray of 500 g capacity which was placed in the drying chamber. The tests were conducted at different allowable *RH* (7, 12, and 17%) and mass flow rates (0.008, 0.012 and 0.016 kg $s^{-1}$) of the recirculating air. The fresh air flow rate, when it was needed, remained constant (around 0.012 kg $s^{-1}$) for all of the tests. Before starting the measurements at each experiment, the dryer was run without load for about 1 hour to reach a steady state condition at the adjusted drying air treatment.

The initial moisture content of the products was determined using oven method. Six temperature sensors (LM35) were used to measure ambient, inlet, and outlet of the solar collector, before the product tray, exhaust air from the drying chamber and the heat exchanger outlet temperatures. To determine the weight variations of the products during the process, two load cells (L6D, Zemic Co., China) were installed in the drying chamber where the product tray was placed on them. Solar radiation intensity on the collector surface was measured using a solar power meter (TES 1333, TES Co., Taiwan) installed on the collector frame. To measure the electrical energy consumed by the auxiliary heater and the fans during the process, a watt meter transmitter (TM 1510, Tika Co., Iran) was employed.

The drying air flow rate (including: fresh and recirculating air) was measured by a digital anemometer (BE816A, Bestone Co., China). A RH sensor (TMH-1, Tika Co., Iran) was located above the product tray to measure *RH* of the drying air. An on/off controller was applied to control the *RH* by activating the external fan when *RH* of the recirculating air reached the set point. The controller system did not allow drying air humidity to exceed the set point by mixing the moist recirculating air with fresh air. The

location of various measuring instruments is shown in Figure 1.

Drying air temperature controller system consisted of an AVR controller which activated the auxiliary electric heater when drying air temperature (measured by the temperature sensor installed before the product tray) fell down below the set point (65$^{o}$C).

## Uncertainty Analysis

Errors and uncertainties in the experiments usually occurr due to instrument, environment, observation and reading, test planning and conditions. To determine total errors and uncertainties incorporated in the experimental measurements, an uncertainty analysis was carried out using the method described by Holman (1994). Based on this method, which was used by many researchers (Mortezapour *et al.*, 2014; Tiwari and Tiwari, 2016), total uncertainty can be calculated as follows:

$$W_{total} = [(x_1)^2 + (x_2)^2) + \cdots + (x_n)^2]^{\frac{1}{2}} \quad (6)$$

Where, $W_{total}$ and $x_n$ are total uncertainty and relative uncertainty of the $n^{th}$ factor, respectively.

The measured parameters in this study were temperature, relative humidity, solar radiation intensity, weight of product, air velocity, and power of the electrical devices. The result of uncertainty analysis is shown in Table 1.

## Parameters Calculation

To investigate the dryer performance, some parameters were calculated as the performance indicators using the data obtained from the experiments. The parameters include efficiency of the open-duct heat recovery system, collector efficiency, total energy consumption, specific energy consumption, solar fraction as well as drying time. Description and calculation method of the parameters are given as follows:

Recovery efficiency of the open duct system indicates the percentage of available thermal energy of the exhaust air that is recycled in the heat exchanger. The efficiency can be calculated as:

$$\zeta_r = \frac{(T_{Ci} - T_{Xi})}{(T_{do} - T_a)} \times 100 \quad (7)$$

Energy used during the drying process includes useful thermal energy generated in the solar collector and electrical energy applied for the auxiliary heater. Electrical energy was measured directly by the wattmeter transmitter installed on the dryer. Solar thermal energy and collector efficiency can be expressed as follows (Singh and Kumar, 2013):

$$E_s = \sum \dot{m_{da}} C_a (T_{coj} - T_{cij}) t \quad (8)$$

**Table 1.** Total uncertainties of the measured variables.

| Parameter | Description | Total uncertainty |
|---|---|---|
| Temperature ($^{o}$C) | Drying air temperature | ±0.51 |
| | Ambient temperature | ±0.51 |
| Relative humidity (%) | Relative humidity of ambient | ±0.31 |
| | Relative humidity of drying air | ±0.31 |
| Air velocity (m s$^{-1}$) | Drying air velocity | ±0.54 |
| Weight (g) | Product weight | ±0.14 |
| Power (W) | Electrical power needed for auxiliary heater and fans | ±1.1 |
| Solar irradiance (W m$^{-2}$) | Solar irradiance on collector surface | ±10 |

$$\zeta_c = \frac{\dot{m}_{da} C_a (T_{coj} - T_{cij})}{A_c I_t} \times 100 \quad (9)$$

Specific energy consumption (SEC) is defined as the thermal energy used to evaporate unit mass of the product moisture and is given as (Singh and Kumar, 2013):

$$SEC = \frac{E_{total}}{[m_d (M_f - M_i)]} \quad (10)$$

Solar fraction (SF) represents the percentage of total energy requirement which is contributed by solar collector, so, it can be expressed as (Mortezapour *et al.*, 2012):

$$SF = \frac{E_s}{E_{total}} \times 100 \quad (11)$$

### Measurement of Visual Colour

Surface colour of the onion slices was measured using a Hunter colourimeter (TES 135A, TES Co., Taiwan). Hunter CIE $L^*$ (lightness/darkness), $a^*$ (redness/greenness) and $b^*$ (yellowness/blueness) were determined, and converted into total colour difference $\Delta E$ and Browning Index *BI*. The $\Delta E$, which indicates the magnitude of colour change after treatment (Bai *et al.*, 2013; Pathare *et al.*, 2013; Tello-Ireland *et al.*, 2011; Wang *et al.*, 2014) was calculated as:

$$\Delta E = [(\Delta L)^2 + (\Delta a)^2 + (\Delta b)^2]^{1/2} \quad (12)$$

The browning index was calculated using the following expression (Pathare *et al.*, 2013).

$$BI = 100.\left(\frac{X - 0.31}{0.17}\right) \quad (13)$$

Where,

$$X = \frac{(a^* + 1.75L)a}{(5.645L + a^* - 3.012b^*)} \quad (14)$$

## RESULTS AND DISCUSSION

### Ambient Conditions

Variations of solar radiation intensity, temperature, and relative humidity of ambient air in a typical day of the experiments are indicated in Table 2. During the test period, solar radiation intensity on the collector surface was between 646 and 1,010 W $m^{-2}$ and ambient air temperature and relative humidity varied between 21-35°C and 12-15%, respectively. The maximum value of solar irradiance was observed at noon and the highest ambient temperature occurred around 2:30 pm.

### Recovery Efficiency of the Open Duct System and Collector Efficiency

It is obvious that the fresh air temperature increases when passing through the heat exchanger. Figure 3 indicates the effect of different exhaust air temperature on temperature rise of the fresh air during the day. As expected, the air temperature rise is higher at the higher exhaust air temperatures. The observations indicated that the average air temperature rise at the exhaust air temperature of 75°C was 2.28°C more than that at 55°C.

Also, Figure 3 shows recovery efficiency of the open-duct system at the different exhaust air temperatures. Although temperature of the inlet air increased with increasing the exhaust air temperature, recovery efficiency was noticeably lower at the higher exhaust air temperatures. The reason is that heat losses from the duct and the heat exchanger to the ambient enhanced at the higher temperatures, mainly due to increase in the temperature gradient between the exhaust air and surrounding atmosphere.

**Table 2.** Hourly variation of solar radiation intensity, ambient relative humidities (RH) and temperature for a typical day of experiment.

| Time | Solar irradiance (W $m^{-2}$) | Ambient temperature ($^oC$) | Ambient RH (%) |
|---|---|---|---|
| 9:00 | 673 | 21 | 15 |
| 9:30 | 750 | 23 | 14 |
| 10:00 | 867 | 26 | 13 |
| 10:30 | 908 | 27 | 12 |
| 11:00 | 974 | 28 | 13 |
| 11:30 | 998 | 29 | 12 |
| 12:00 | 1010 | 31 | 13 |
| 12:30 | 1005 | 32 | 13 |
| 13:00 | 965 | 33 | 12 |
| 13:30 | 968 | 34 | 12 |
| 14:00 | 891 | 34 | 13 |
| 14:30 | 798 | 35 | 12 |
| 15:00 | 646 | 34 | 13 |

However, average recovery efficiencies of 36, 33, and 31% were achieved at the exhaust air temperatures of 55, 65 and 75°C, respectively.

Hourly variations of collector efficiency at the different exhaust air temperatures are shown in Figure 4. One of the most effective factors on the collector efficiency is its inlet temperature. Increasing of the inlet temperature more than ambient leads to a fall in efficiency (Duffie and Beckman, 2006). In the present study, since collector inlet temperature was higher at the higher exhaust air temperatures (as mentioned above), collector efficiency reasonably decreased with the increase of exhaust air temperature. According to Figure 4, it can be expressed that average collector efficiency at the exhaust air temperature of 55°C is 3.94% better than that at 75$^o$C.

## Drying Time

Variation of drying time at different drying air conditions is illustrated in Figure 5. Although some researchers (Koukouch *et al.*, 2015; Mortezapour *et al.*, 2012; Udomkun *et al.*, 2015) have concluded that drying rate increases with air flow rate, Figure 5 indicates that drying time is longer at the higher velocities of the recirculating air. This stems from the fact that in the designed dryer, temperature of the recirculating air after passing over the solar collector rises much more at lower air flow rates. On the other hands, it can be concluded that drying air temperature is higher with applying lower air flow rates, which enhances drying rate. This finding is in accordance with the results of Arslan and Musa Özcan (2010) and Nowak and Lewicki (2004).

It is clear from Figure 5 that drying period is longer at the higher relative humidities. With increase in the *RH* from 7 to 17%, drying time increased by 10%. This is because of reducing the vapour pressure difference between drying air and product, which subsequently led to a decrease in moisture removal potential at the higher humidities. Similar result was obtained by Sarsavadia (2007).

Variation of drying air *RH* at different allowable relative humidities is shown in Figure 6. Clearly, after placing the product tray in the drying chamber (time 0), the *RH* rises abruptly due to considerable evaporation rate of free water from the product surface. The peak values on the diagram indicate that the external fan was activated to replace a part of moist air with fresh air, and it was effectively able to drop the *RH* below the lower set point where the external fan turns off again. This process repeated 3 or 5 times during each test and,

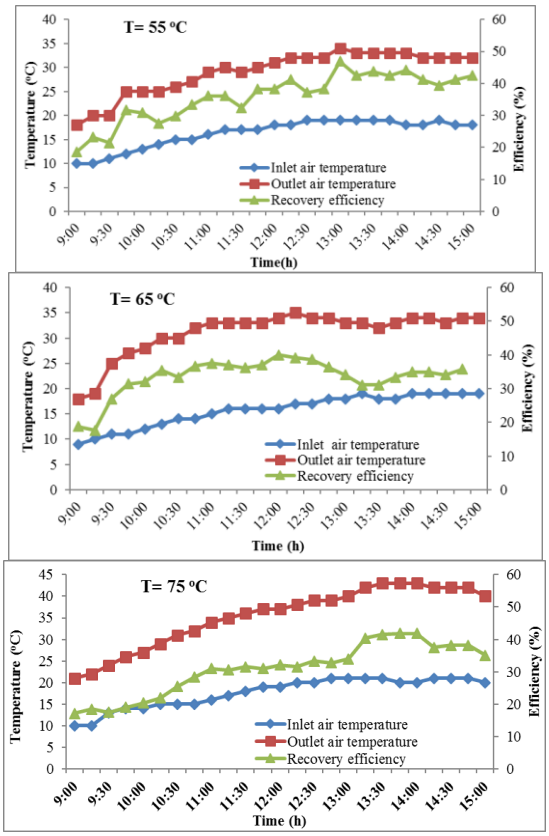


**Figure 3.** Recovery efficiency and temperature rise of the fresh air at different exhaust air temperatures.

afterwards, the *RH* plateaus while the external fan remains inactivated. Figure 5 also illustrates that time duration of the external fan activation is lower and, consequently, *RH* of drying air during the drying process is higher at higher adjusted relative humidities. Totally, it can be deduced from the observations that the external fan was activated for about 25, 38, and 51 minutes at adjusted maximum relative humidities of 17, 12, and 7%, respectively.

## Energy Consumption

Figure 7 shows the required electrical energy for onion drying in different conditions. It is obvious from Figure 7 that increasing the *RH* from 7 to 17% caused a reduction of 51% in electrical energy consumption. Since a larger fraction of drying air is recycled with applying higher relative humidities, the electric heater is off for a longer time, which leads to a lower energy consumption. The results also indicated that required electrical energy increased by 24% with rise in the air flow rate from 0.008 to 0.016 kg $s^{-1}$. These findings are in agreement with the results of Sarsavadia (2007).

Solar fraction is highly influenced by solar collector efficiency and drying time. Increasing the RH causes a longer drying time which results in achieving higher solar fraction. Vice versa, at the higher relative humidities, a larger fraction of the drying air is recycled, which leads to a reduction in solar collector efficiency and solar fraction. This is probably why solar fraction decreased when the *RH* increased from 7 to 12%, and improved when the *RH* increased to 17% (Figure 8). Increasing the air flow rate enhances collector efficiency and increases drying time, both of which cause an improvement in solar fraction. The results indicated a growth of 7% in solar fraction with rise in the air flow rate from 0.008 to

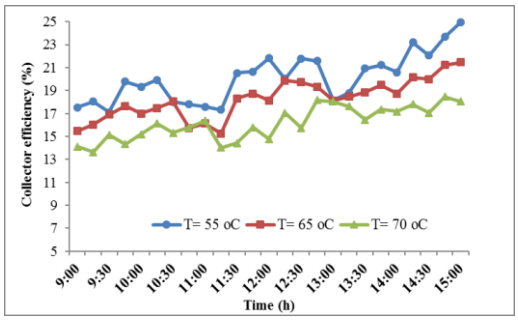


**Figure 4.** Hourly variations of collector efficiency at different exhaust air temperatures.

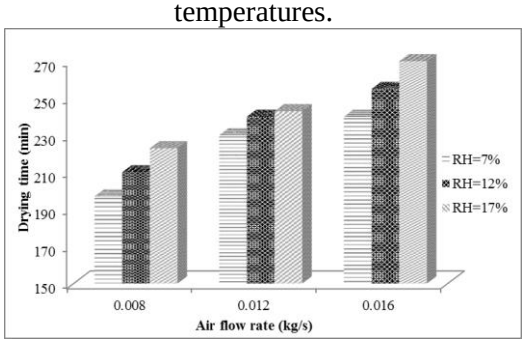


**Figure 5.** Variation of drying time in different drying conditions.

0.016 kg $s^{-1}$. A maximum solar fraction value of 25.1% was achieved at the air flow rate of 0.016 kg $s^{-1}$ and the *RH* of 17%.

The effect of various drying conditions on specific energy consumption is demonstrated in Figure 9. The required energy decreased with increasing the *RH*, fundamentally owing to using more fractions of recycled air. The results also indicate that as the air flow rate rises, the energy consumption increases, probably because a larger volume of drying air needs to be warmed for a longer period at the higher air flow rates. Similar results were reported previously (Darvishi *et al.*, 2013; Motevali *et al.*, 2012; Singh and Kumar, 2013). The lowest *SEC* value was found to be 7.54 MJ $kg^{-1}$ at the highest *RH* and the lowest air flow rate. Sarsavadia (2007) achieved a minimum *SEC* of 12 MJ $kg^{-1}$ when drying onion slices at the lowest air flow rate and the highest fraction of recycled air.

## Colour Change

The flavour, taste, colour, and nutrients may be affected substantially by drying process (Arslan and Özcan, 2011). Colour is an important factor in the perception of food products quality and is affected by the enzymatic and non-enzymatic browning (Pathare *et al.*, 2013). The product colour is the quality parameter that should be maintained during onion drying (Arslan and Özcan, 2011).

Table 3 shows the changes in surface colour of the onion slices dried at various air flow rates (0.008-0.016 kg $s^{-1}$) and relative humidities (7-17%), as given by *L** (lightness/darkness), *a** (redness/greenness) and *b** (yellowness/blueness), *ΔE* and *BI*. The results showed that the colour indices changed during onion slices drying. The colour indices variations were dependent upon the flow rate, *RH* and, consequently, drying time. Higher *L** values are desirable in the dried products, as the lower *L** and higher *BI* values showed a darkening tendency in the surface colour.

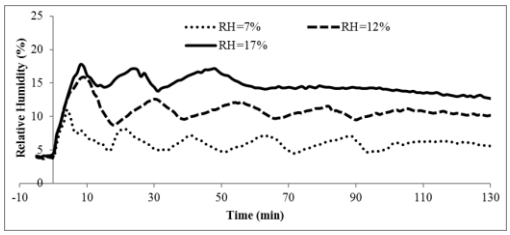


**Figure 6.** Variation of drying air *RH* at the flow rate of 0.012 kg $s^{-1}$.

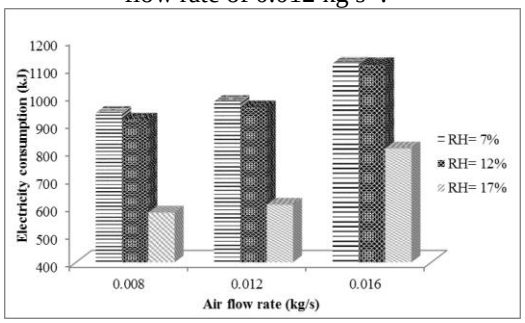


**Figure 7.** Variation of electrical energy consumption in different drying conditions.

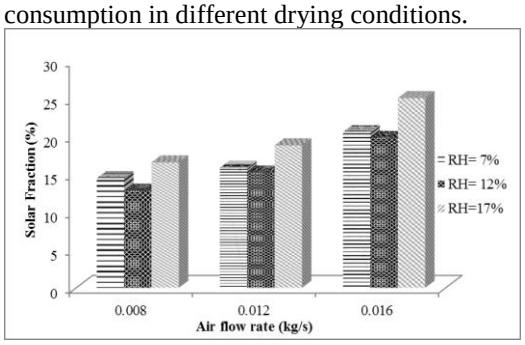


**Figure 8.** Variation of solar fraction in different drying conditions.

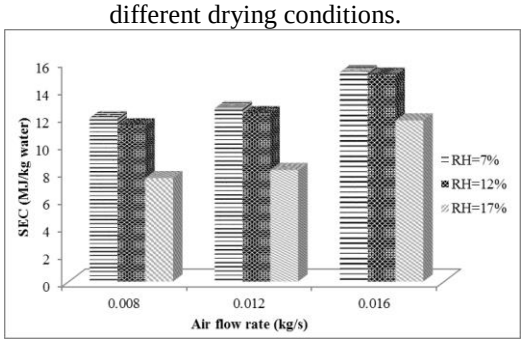


**Figure 9.** Variation of specific energy consumption in different drying conditions.

Also, the *ΔE* indicates the magnitude of colour change after treatment (Pathare *et al.*, 2013).

In a constant *RH*, reduction of the air flow rate from 0.016 to 0.008 kg $s^{-1}$ led to an increasing trend in *L** and decreasing trends of *a**, *b**, *ΔE* and *BI*. These results indicate that low air flow rate could maintain better colour

**Table 3.** Changes in surface colour (*L**, *a**, *b**, total colour difference (*ΔE*) and Browning Index (*BI*)) of onion slices dried in different drying conditions.

| | Time (min) | Velocity (kg $s^{-1}$) | *RH* (%) | *L** | *a** | *b** | *ΔE* | *BI* |
|---|---|---|---|---|---|---|---|---|
| Control | 0 | 0 | 0 | 65.37±0.3 | -1.20±0.1 | 5.40±0.2 | 0.00 | 6.98±0.32 |
| S1 | 240 | 0.016 | 7 | 49.49±2.8 | 3.45±0.3 | 16.11±1.5 | 19.75±2.8 | 43.58±5.9 |
| S2 | 230 | 0.012 | 7 | 50.09±2.7 | 3.20±0.1 | 16.53±0.6 | 19.44±2.4 | 43.66±4.2 |
| S3 | 197 | 0.008 | 7 | 55.98±3.3 | 1.77±0.2 | 15.12±1.4 | 14.06±2.4 | 32.92±3.7 |
| S4 | 255 | 0.016 | 12 | 49.71±3.7 | 3.04±0.4 | 16.95±1.3 | 20.03±2.8 | 45.11±4.9 |
| S5 | 240 | 0.012 | 12 | 57.97±4.3 | 2.92±0.5 | 16.52±0.7 | 14.43±1.9 | 36.36±3.1 |
| S6 | 210 | 0.008 | 12 | 58.92±4.3 | 0.84±0.1 | 16.33±1.0 | 13.34±2.4 | 32.75±4.8 |
| S7 | 270 | 0.016 | 17 | 51.39±2.9 | 3.74±0.4 | 18.60±1.1 | 19.94±2.5 | 49.19±5.9 |
| S8 | 243 | 0.012 | 17 | 61.01±3.3 | 2.41±0.3 | 17.46±0.5 | 13.66±1.4 | 35.62±2.3 |
| S9 | 223 | 0.008 | 17 | 63.64±3.9 | 0.73±0.1 | 16.74±1.5 | 12.25±1.3 | 30.28±1.1 |

indices due to shorter drying time. Furthermore, at a constant velocity, increasing the *RH* from 7 to 17% increased *L** and *b** and decreased *a*, ΔE* and *BI.* Although, the rise in the *RH* increased drying time, it could make an improvement in colour indices, indicating the positive effect of 17% humidity compared to 7%. Generally, it can be stated that the lower velocities and the higher *RH* resulted in better lightness and decreased browning of dried onions.

The long drying time as well as high temperature can reduce the product quality due to caramelisation, Maillard reactions, enzymatic reactions, pigment degradation, and *L*-ascorbic acid oxidation (Arslan and Özcan, 2011). The result showed that the good appearance qualities of dried onion were achieved at the higher *RH*. It seems that increasing the *RH* reduced the case-hardening, which usually occurs if the drying rate is too high. Therefore, the internal moisture was allowed sufficient time to diffuse to the surface and prevent surface against a rapid rise in temperature, which reduces the product colour change (Chua *et al.*, 2001).

## CONCLUSIONS

The performance investigation of a solar dryer equipped with a novel heat recovery system was considered in the present study. The evaluation tests were conducted at different levels of flow rate and allowable *RH* of the drying air. The results can be summarized as follows: Drying time increased by 10% as the *RH* increased from 7 to 17%, respectively. The highest solar fraction value was found to be 25.1% which was achieved at the air flow rate of 0.016 kg $s^{-1}$ and the *RH* of 17%. Specific energy consumption improved with reduction in the air flow rate and increase in the *RH*. A minimum *SEC* value of 7.54 MJ $kg^{-1}$ was observed at the highest *RH* and the lowest air flow rate. The colour indices variations were dependent upon the air flow rate, *RH*, and consequently, drying time. The colour indices of dried onions were improved at the lower air flow rates and higher *RH*.

## NOMENCLATURE

| | |
|---|---|
| a* | Redness/Greenness index |
| $A_c$ | Collector area ($m^2$) |
| $A_{HE}$ | Total surface area (fin plus exposed base) of the heat exchanger ($m^2$) |
| $A_i$ | Inner tube surface area ($m^2$) |
| b* | Yellowness/Blueness index |
| BI | Browning index |
| $C_a$ | Specific heat of drying air (J $kg^{-1}$ $K^{-1}$) |
| $D_i$ | Inner diameter of heat exchanger tube (m) |

| | |
|---|---|
| $D_o$ | Outer diameter of heat exchanger tube (m) |
| $E_s$ | Solar thermal energy (J) |
| $E_{total}$ | Total energy consumption (kJ) |
| ΔE | Colour change after treatment |
| $F_R$ | Collector heat removal factor |
| $h_a$ | Convection coefficient of fresh air around the fines (W $m^{-2}$ $K^{-1}$) |
| $h_{da}$ | Enthalpy of drying air (J $kg^{-1}$) |
| $h_e$ | Convection coefficient of exhaust air through the tube (W $m^{-2}$ $K^{-1}$) |
| $I_t$ | Solar radiation intensity (W $m^{-2}$) |
| $K_m$ | Thermal conductivity of heat exchanger (W $m^{-1}$ $K^{-1}$) |
| L* | Lightness/darkness index |
| $L_t$ | Length of heat exchanger tube (m) |
| $\dot{m}_a$ | Mass flow rate of fresh air (kg $s^{-1}$) |
| $m_d$ | Dry matter mass of product (kg) |
| $\dot{m}_{da}$ | Mass flow rate of drying air through the collector (kg $s^{-1}$) |
| $\dot{m}_r$ | Mass flow rate of recirculating air (kg $s^{-1}$) |
| $M_f$ | Final moisture content of product (kg water $kg^{-1}$ dry matter) |
| $M_i$ | Initial moisture content of product (kg water $kg^{-1}$ dry matter) |
| $\dot{q}_{HE}$ | Rate of heat transfer in the heat exchanger (W) |
| $SEC$ | Specific energy consumption (kj $kg^{-1}$) |
| $SF$ | Solar fraction (%) |
| $T_a$ | Ambient temperature ($^oC$) |
| $T_{Ci}$ | Temperatures of the collector inlet ($^oC$) |
| $T_{cij}$ | The *j* th collector inlet temperature ($^oC$) |
| $T_{coj}$ | The *j* th collector outlet temperature ($^oC$) |
| $T_i$ | Inlet fluid temperature ($^oC$) |
| $T_{od}$ | Outlet temperature of drying chamber ($^oC$) |
| $T_{xi}$ | Fresh-air intake temperature of the heat exchanger ($^oC$) |
| $\Delta T_c$ | Temperature rise through the collector ($^oC$) |
| $\Delta T_{lm}$ | Log mean temperature difference ($^oC$) |
| $U_{HE}$ | Overall heat transfer coefficient (W $m^{-2}$ $K^{-1}$) |
| $U_L$ | Collector overall heat losses coefficient (W $m^{-2}$) |
| $Wi$ | Error of the $i^{th}$ factor (%) |
| $W_{total}$ | Total Uncertainty (%) |
| $\alpha$ | Absorption coefficient of absorber plate |
| $\tau$ | Transmission coefficient of glass |
| $\omega_a$ | Humidity ratio of fresh air (kg water $kg^{-1}$ dry air) |
| $\omega_m$ | Humidity ratio of mixture (kg water $kg^{-1}$ dry air) |
| $\omega_{od}$ | Humidity ratio at the outlet of drying chamber (kg water $kg^{-1}$ dry air) |
| $\omega_r$ | Humidity ratio of recirculating air (kg water $kg^{-1}$ dry air) |
| $\zeta_f$ | Temperature effectiveness of the finned surface (Decimal) |
| $\zeta_c$ | Solar collector efficiency (%) |
| $\zeta_r$ | Recovery efficiency (%) |
| $\dot{q}_{HE}$ | Rate of heat transfer in the heat exchanger (W) |

## REFERENCES


1. Aktaş, M., Şevik, S., Özdemir, M. B. and Gönen, E. 2015. Performance Analysis and Modeling of a Closed-loop Heat Pump Dryer for Bay Leaves Using Artificial Neural Network. *Appl. Therm. Eng.*, **87:** 714-723.
2. Arslan, D. and Özcan, M. M. 2010. Study the Effect of Sun, Oven and Microwave Drying on Quality of Onion Slices. *LWT - Food Sci.Technol.*, **43(7):** 1121-1127.
3. Arslan, D. and Özcan, M. M. 2011. Dehydration of Red Bell-Pepper (*Capsicum annuum* L.): Change in Drying Behavior, Colour and Antioxidant Content. *Food Bioprod. Process.*, **89(4):** 504-513.
4. Bai, J.-W., Sun, D. -W., Xiao, H. -W., Mujumdar, A. S. and Gao, Z.-J. 2013. Novel High-Humidity Hot Air Impingement Blanching (HHAIB) Pretreatment Enhances Drying Kinetics and Color Attributes of Seedless Grapes. *Innov. Food Sci. Emerg. Technol.*, **20:** 230-237.
5. Brooker, D. B., Bakker-Arkema, F. W. and Hall, C. W. 1992. *Drying and Storage of Grains and Oilseeds*. Springer.
6. Chua, K. J., Mujumdar, A. S., Hawlader, M. N. A., Chou, S. K. and Ho, J. C. 2001. Batch Drying of Banana Pieces: Effect of Stepwise Change in Dying Air Temperature on Drying

Kinetics and Product Colour. *Food Res. Int.*, **34(8):** 721-731.
7. Darvishi, H., Khoshtaghaza, M., Najafi, G. and Nargesi, F. 2013. Mathematical Modeling of Green Pepper Drying in Microwave-Convective Dryer. *J. Agric. Sci. Technol.*, **15(3):** 457-465.
8. Das, S., Das, T., Srinivasa Rao, P. and Jain, R. K. 2001. Development of an Air Recirculating Tray Dryer for High Moisture Biological Materials. *J. Food Eng.*, **50(4):** 223-227.
9. Dina, S. F., Ambarita, H., Napitupulu, F. H. and Kawai, H. 2015. Study on Effectiveness of Continuous Solar Dryer Integrated with Desiccant Thermal Storage for Drying Cocoa Beans. *Case Stud. Therm. Eng.*, **5:** 32-40.
10. Duffie, J. A. and Beckman, W. A. 2006. *Solar Engineering of Thermal Processes.* Wiley-Interscience, New York.
11. Elkhadraoui, A., Kooli, S., Hamdi, I. and Farhat, A. 2015. Experimental Investigation and Economic Evaluation of a New Mixed-Mode Solar Greenhouse Dryer for Drying of Red Pepper and Grape. *Renew. Ener.*, **77:** 1-8.
12. Fudholi, A., Sopian, K., Alghoul, M. A., Ruslan, M. H. and Othman, M. Y. 2015. Performances and Improvement Potential of Solar Drying System for Palm Oil Fronds. *Renew. Ener.*, **78:** 561-565.
13. Gudiño-Ayala, D. and Calderón-Topete, Á. 2014. Pineapple Drying Using a New Solar Hybrid Dryer. *Ener. Procedia*, **57:** 1642-1650.
14. Holman, J. 1994. *Experimental Methods for Engineers*. 2nd Edition, Mcgraw-Hill. New York, PP. 41-49.
15. Hossain, M. A., Gottschalk, K. and Hassan, M. S. 2013. Mathematical Model for a Heat Pump Dryer for Aromatic Plant. *Procedia Eng.*, **56:** 510-520.
16. Incropera, F. and DeWitt, D. 1996. *Introduction to Heat Transfer*. John Wiley, New York.
17. Jain, D. and Tewari, P. 2015. Performance of Indirect through Pass Natural Convective Solar Crop Dryer with Phase Change thermal Energy Storage. *Renew. Ener.*, **80:** 244-250.
18. Koukouch, A., Idlimam, A., Asbik, M., Sarh, B., Izrar, B., Bah, A. and Ansari, O. 2015. Thermophysical Characterization and Mathematical Modeling of Convective Solar Drying of Raw Olive Pomace. *Ener. Convers. Manage.*, **99:** 221-230.
19. Mortezapour, H., Ghobadian, B., Khoshtaghaza, M. and Minaei, S. 2014. Drying Kinetics and Quality Characteristics of Saffron Dried with a Heat Pump Assisted Hybrid Photovoltaic-Thermal Solar Dryer. *J. Agr. Sci. Tech.*, **16(1):** 33-45.
20. Mortezapour, H., Ghobadian, B., Minaei, S. and Khoshtaghaza, M. H. 2012. Saffron Drying with a Heat Pump–Assisted Hybrid Photovoltaic–Thermal Solar Dryer. *Dry. Technol.*, **30(6):** 560-566.
21. Motevali, A., Abbaszadeh, A., Minaei, S., Khoshtaghaza, M. and Ghobadian, B. 2012. Effective Moisture Diffusivity, Activation Energy and Energy Consumption in Thin-Layer Drying of Jujube (*Zizyphus jujube* Mill). *J. Agr. Sci. Tech.*, **14(3):** 523-532.
22. Nowak, D. and Lewicki, P. P. 2004. Infrared Drying of Apple Slices. *Innov. Food Sci. Emerg. Technol.*, **5(3):** 353-360.
23. Pathare, P. B., Opara, U. L. and Al-Said, F. A.-J. 2013. Colour Measurement and Analysis in Fresh and Processed Foods: A Review. *Food Bioprocess Tech.*, **6(1):** 36-60.
24. Punlek, C., Pairintra, R., Chindaraksa, S. and Maneewan, S. 2009. Simulation Design and Evaluation of Hybrid PV/T Assisted Desiccant Integrated HA-IR Drying System (HPIRD). *Food Bioprod. Process.*, **87(2):** 77-86.
25. Ringeisen, B., M. Barrett, D. and Stroeve, P. 2014. Concentrated Solar Drying of Tomatoes. *Ener. Sustain. Dev.*, **19:** 47-55.
26. Sarsavadia, P. N. 2007. Development of a Solar-Assisted Dryer and Evaluation of Energy Requirement for the Drying of Onion. *Renew. Ener.*, **32(15):** 2529-2547.
27. Şevik, S. 2014. Experimental Investigation of a New Design Solar-Heat Pump Dryer under the Different Climatic Conditions and Drying Behavior of Selected Products. *Solar Ener.*, **105:** 190-205.
28. Shalaby, S. M. and Bek, M. A. 2014. Experimental Investigation of a Novel Indirect Solar Dryer Implementing PCM as Energy Storage Medium. *Ener. Convers. Manage.*, **83:** 1-8.
29. Shanmugam, V. and Natarajan, E. 2007. Experimental Study of Regenerative Desiccant Integrated Solar Dryer with and without Reflective Mirror. *Appl. Therm. Eng.*, **27(8–9):** 1543-1551.
30. Singh, S. and Kumar, S. 2013. Solar Drying for Different Test Conditions: Proposed Framework for Estimation of Specific Energy

Consumption and $CO_2$ Emissions Mitigation. *Ener.*, **51:** 27-36.
31. Tello-Ireland, C., Lemus-Mondaca, R., Vega-Gálvez, A., López, J. and Di Scala, K. 2011. Influence of Hot-Air Temperature on Drying Kinetics, Functional Properties, Colour, Phycobiliproteins, Antioxidant Capacity, Texture and Agar Yield of Alga *Gracilaria chilensis*. *LWT - Food Sci. Technol.*, **44(10):** 2112-2118.
32. Tiwari, S. and Tiwari, G. N. 2016. Thermal Analysis of Photovoltaic-Thermal (PVT) Single Slope Roof Integrated Greenhouse Solar Dryer. *Solar Ener.*, **138:** 128-136.
33. Türk Toğrul, İ. and Pehlıvan, D. 2003. The Performance of a Solar Air Heater with Conical Concentrator under Forced Convection. *Int. J. Therm. Sci.*, **42(6):** 571-581.
34. Udomkun, P., Argyropoulos, D., Nagle, M., Mahayothee, B., Janjai, S. and Müller, J. 2015. Single Layer Drying Kinetics of Papaya Amidst Vertical and Horizontal Airflow. *LWT - Food Sci. Technol.*, **64(1):** 67-73.
35. Wang, Y., Tao, H., Yang, J., An, K., Ding, S., Zhao, D. and Wang, Z. 2014. Effect of Carbonic Maceration on Infrared Drying Kinetics and Raisin Qualities of Red Globe (*Vitis vinifera* L.): A New Pre-Treatment Technology before Drying. *Innov. Food Sci. Emerg. Technol.*, **26:** 462-468.
36. Wannapakhe, S., Chaiwong, T., Dandee, M. and Prompakdee, S. 2012. Hot Air Dryer with Closed–Loop Oscillating Heat Pipe with Check Valves for Reducing Energy in Drying Process. *Procedia Eng.*, **32:** 77-82.
37. Zomorodian, A. and Barati, M. 2010. Efficient Solar Air Heater with Perforated Absorber for Crop Drying. *J. Agr. Sci. Tech.*, **12:** 569-577.

## بررسی تجربی یک خشک کن خورشیدی مجهز به سامانه بازیافت حرارتی جدید برای خشک کردن پیاز

**ح. مرتضی پور، س. ج. راشدی، ح. ر. اخوان و ح. مقصودی**

### چکیده

در خشک‌کن‌های هوای گرم سهم کوچکی از گرمای تأمین شده، صرف خشک کردن محصول می-شود و بخش زیادی از آن به همراه جریان هوا به بیرون خشک‌کن منتقل می‌گردد. به منظور بازیافت حرارت از جریان هوای خروجی، در تحقیق حاضر، یک خشک‌کن خورشیدی مجهز به سامانه بازیافت حرارتی جدید پیشنهاد شد. خشک‌کن طراحی شده از جمع‌کننده خورشیدی، محفظه خشک‌کن، سامانه سیکل بسته هوای داخلی و سامانه بازیافت گرمای با مدار باز تشکیل شده است. آزمایش‌های ارزیابی خشک‌کن در سه سطح دبی و رطوبت نسبی هوای خشک‌کننده انجام شد. نتایج نشان داد که زمان خشک کردن با افزایش رطوبت نسبی هوا افزایش یافت. بهترین سهم خورشیدی در بالاترین رطوبت نسبی و دبی مشاهده شد. افزایش رطوبت نسبی از ۷ تا ۱۷ درصد باعث کاهش مصرف جریان الکتریسیته به میزان ۵۱٪ گردید. همچنین با بالا رفتن دبی هوا از ۰/۰۰۸ به ۰/۰۱۶ **کیلوگرم/ثانیه** انرژی الکتریکی مورد نیاز به میزان ۲۴٪ افزایش یافت. کمترین مصرف ویژه انرژی به مقدار ۷/۵۴ **مگا ژول/کیلوگرم** در بالاترین رطوبت نسبی و کمترین دبی هوا حاصل شد. در رطوبت نسبی ثابت، کاهش

دبی هوا از ۰/۰۱۶ تا ۰/۰۰۸ منجر به روند افزایشی در روشنی و روند کاهشی شاخص قهوه‌ای شدن شد. به علاوه، افزایش رطوبت نسبی از ۷ تا ۱۷٪ باعث افزایش روشنی و کاهش شاخص قهوه‌ای شدن گردید. به طور کلی، می‌توان نشان داد که بهترین کیفیت رنگ هنگام استفاده از کمترین دبی هوا و بیشترین رطوبت نسبی در خشک‌کن خورشیدی حاصل می‌گردد.